NANO LETTERS

2007
Vol. 7, No. 8
2243−2247

Direct Observation of Field Emission in a Single $TaSi_2$ Nanowire

Joong Jung Kim,† Daisuke Shindo,*,† Yasukazu Murakami,† Weixing Xia,† Li-Jen Chou,‡ and Yu-Lun Chueh‡

Institute of Multidisciplinary Research for Advanced Materials, Tohoku University, Sendai 980-8577, Japan, and Department of Materials Science and Engineering, National Tsing Hua University, Hsinchu, Taiwan, Republic of China

Received March 25, 2007; Revised Manuscript Received May 28, 2007

ABSTRACT

The electric potential change in a single $TaSi_2$ nanowire during field emission was visualized by means of electron holography. During the field emission, the interference fringes of the electron hologram were blurred locally between the $TaSi_2$ nanowire and anode. This phenomenon was interpreted as being due to a change in the electric potential of approximately 1 V in the $TaSi_2$ nanowire after each ballistic emission. The experiments on the single $TaSi_2$ nanowire field emission behavior provide the useful information for understanding the field emission in the nano-field-emitting device.

The field-emission phenomenon has been widely used in various applications such as field-emission displays, X-ray generators, and electron sources for electron microscopes.[1,2] Many researchers have focused not only on the syntheses of new field emitters and their integration with tube/wire shaped nanostructures but also on the theoretical interpretations of the field-emission properties in order to develop a highly efficient field emitter which has a high current density at a lower operation voltage.[2−6] Recently, in situ studies under field-emission conditions have been extensively carried out on electron emitters made of nanotubes and nanowires in order to determine their essential properties.[7−14] However, there are few studies on the changes in the electric potential in a single nanotube/nanowire during field emission, although these studies are important to the understanding of the field-emission process and mechanism.

Electron holography provides a unique method for detecting the phase shift of the electron wave due to an electromagnetic field.[15] Thus, this technique has been considered to be a useful tool for quantitatively visualizing electric and magnetic fields on a nanometer scale.[16−18] On the other hand, in order to precisely evaluate the electric potential distribution by electron holography, particularly in the case of a field-emitting device involving a large electric field, the influence of the reference wave modulated by the leakage field around the specimen should be considered.[17−18]

In this study, the electric potential distribution around a single $TaSi_2$ nanowire[19] in the presence of an applied voltage was analyzed on a nanometer scale by means of electron holography performed at the experimental condition devised for obtaining an unmodulated reference wave.[20]

Electron holography was carried out with a JEM-3000F transmission electron microscope installed with a field-emission gun and a biprism. The exposure time was 6 s. For the direct observation of the field emission in the transmission electron microscope, a single $TaSi_2$ nanowire was mounted on a commercial tungsten needle using a conductive silver paste, as shown in Figure 1a. Another tungsten needle was used as an anode. This pair, comprising the single $TaSi_2$ nanowire and the tungsten anode, was placed in a special specimen holder, in which the spacing between the nanowire and the anode can be controlled by a stepping motor and piezoelectric drives. It is noted that the tungsten anode was positioned in order to prevent the reference wave from being modulated by the applied voltage, as shown in Figure 1b. The $I-V$ curve was measured using a Keithley 6487 picoammeter in a vacuum level of 1.8×10^{-5} Pa.

Panels a−c of Figure 2 show the electron holograms (left panels) and their corresponding reconstructed phase images (right panels) obtained when the applied voltage between the $TaSi_2$ nanowire and tungsten anode is 0, 30, and 50 V, respectively. The digital diffractograms are shown in the center panels. The $I-V$ curve and Fowler−Nordheim (F−N) plot are given in parts d and e of Figure 2. From the $I-V$ curve, it is noted that the field emission starts above 40 V, and the field-emission current increases up to 28 nA at the applied voltage of 100 V. Further, it is clarified that the F−N plot of a $TaSi_2$ nanowire shows a linear relationship, exhibiting a typical field-emission characteristic. By use of

* Corresponding author. E-mail: shindo@tagen.tohoku.ac.jp.
† Tohoku University.
‡ National Tsing Hua University.

10.1021/nl070696v CCC: $37.00
Published on Web 06/28/2007

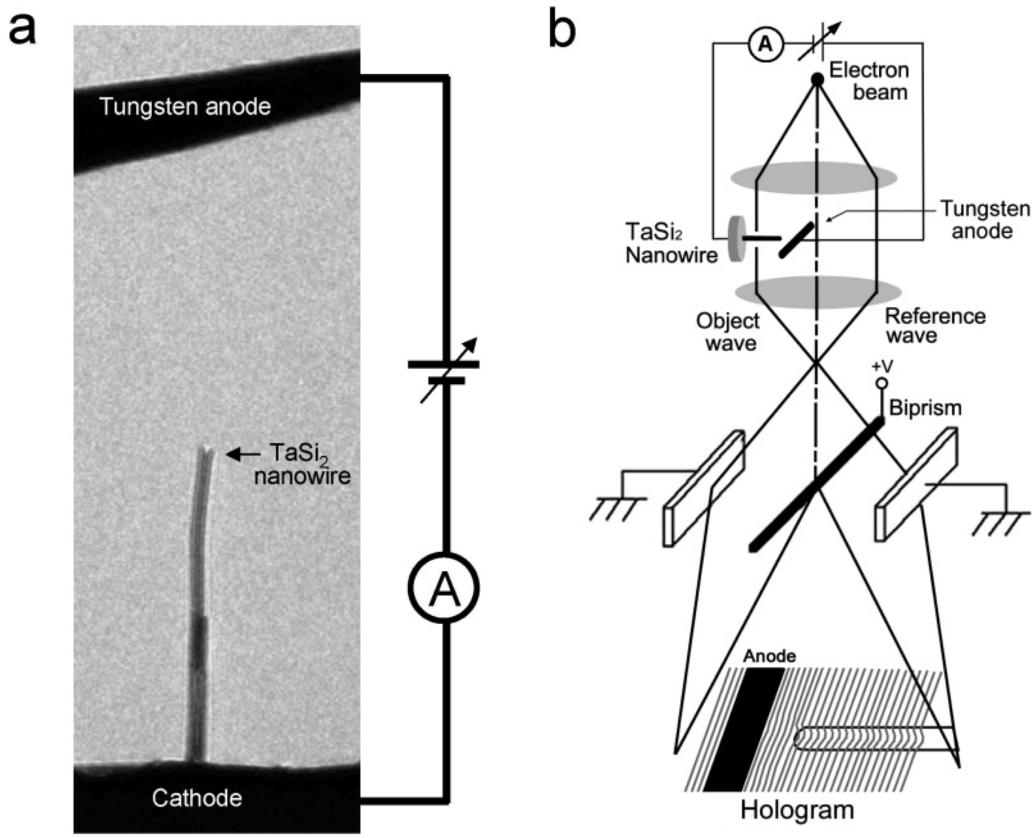

Figure 1. The transmission electron microscope image (a) and the schematic illustration (b) showing the experimental setup.

the slope (k_{F-N}) of the F−N plot, the field enhancement factor in this system is calculated to be approximately 262.

In the reconstructed phase images (right panels in (a−c)), the white and black lines exhibit the equiphase lines formed by electrons passing through an electromagnetic field; in the field-emitting device, these lines indicate the equipotential lines, reflecting the three-dimensional electric potential distribution integrated along the trajectories of the incident electrons.[15] In Figure 2a, when the applied voltage is zero, only the inner potential of the $TaSi_2$ nanowire is observed; in other words, the variation in the electric potential is not observed around the $TaSi_2$ nanowire as well as in the upper region of the tungsten anode. On the other hand, the phase information is poor at the position of the thick tungsten anode due to the absorption of incident electrons. Here, we should note that there is no appreciable variation in the potential distribution in the upper regions of the tungsten anode even at the biased condition shown in panels b and c of Figure 2. These results can be confirmed through the digital diffractograms, i.e., the position of a sideband caused by the zero-field region of Figure 2a is the same as that of the sidebands indicated by the white arrows in panels b and c of Figure 2. This means that the reference wave is unaffected by the applied voltage; i.e., the reference wave is not modulated in this experimental setup.

On the other hand, with an increase in the applied voltage, it can be observed that the additional sidebands indicated by the yellow arrows in the digital diffractograms of panels b and c of Figure 2 are formed, and the distance between the additional sidebands and the sidebands caused by the zero-field region increases. Meanwhile, in the reconstructed phase images of the previous studies,[14,18,20] the gradient of the equipotential lines around a charged tip or an emitter was concentrated at their top edge, indicating the field concentration on their top edge. However, in this study, the reconstructed phase images show that the equipotential lines are observed as almost straight lines. It is noted that the equipotential lines are considered to be contributed by two components. The first one is from the nanowire, and the other one is from the cathode below the nanowire. In this experimental setup, the contribution of a second component is so large compared with the first component and, thus, the equipotential lines are observed as almost straight lines. The distance between the equipotential lines corresponding to a phase shift of 2π (distance between white or black lines) is 13 nm for the applied voltage of 30 V and 8 nm for 50 V. These results indicate that the electric field between the nanowire and anode is very uniform. On the other hand, it is interesting to note that in the case of the applied voltage of 50 V, i.e., the field-emission condition, an irregular contrast in the reconstructed phase image, resulting from the blurring of interference fringes in the corresponding hologram, can be observed between the $TaSi_2$ nanowire and the tungsten anode (indicated by "I") as shown in Figure 2c. These results indicate that an abrupt change occurs in the electric potential during the field emission, while the electric potential distribution is uniformly preserved before the field emission.

Panels a and b of Figure 3 show the electron hologram and the corresponding reconstructed phase image of

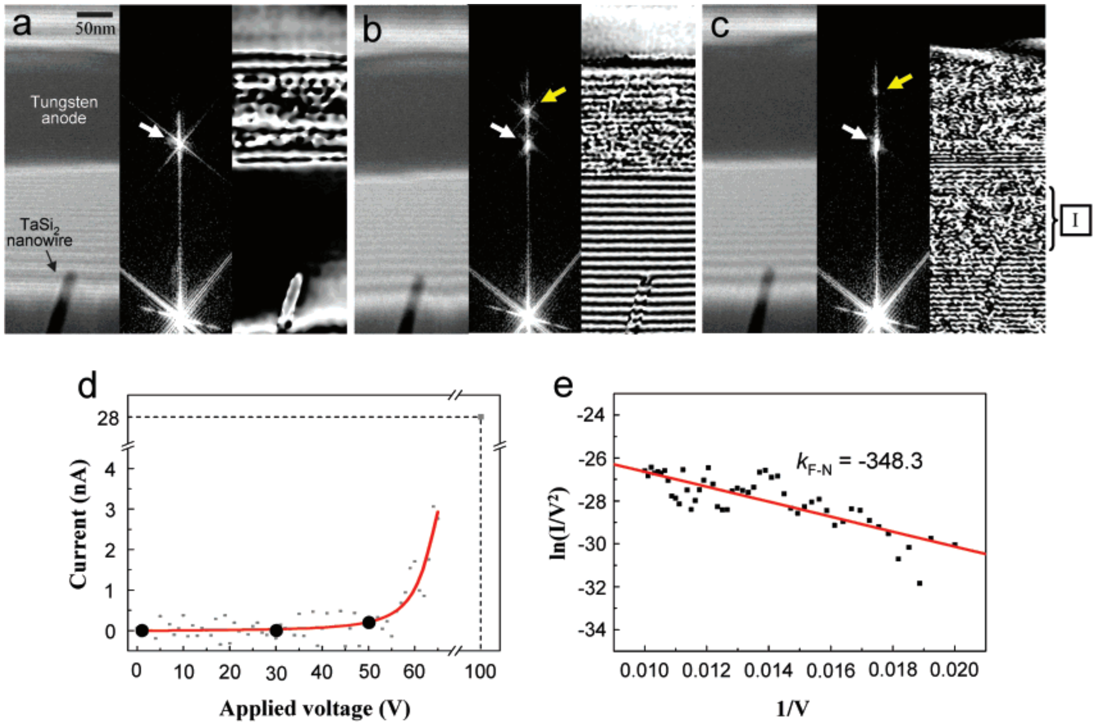

Figure 2. Changes in the electric potential distribution and field-emission current with the applied voltage in a single $TaSi_2$ nanowire field-emitting device. Electron holograms (left image), and their corresponding reconstructed phase images (right image)/digital diffractograms (center image) obtained when the applied voltage between the $TaSi_2$ nanowire and tungsten anode is (a) 0, (b) 30, and (c) 50 V, respectively. White arrows indicate sidebands caused by the zero-field region, and yellow arrows indicate sidebands caused by the applied-field region. The corresponding $I-V$ curve (d) and Fowler−Nordheim plot (e) are also shown.

Figure 2c with an enlarged field of view. The interference fringes extending from the top right to the bottom left of the figure cover a region with a width of approximately 400 nm. The irregular-contrast region with a band shape between the $TaSi_2$ nanowire and anode can be observed more clearly as shown in Figure 3c. In the reconstructed phase image, the intensity $I_{ph}(r)$ is represented by a cosine function with a phase shift $\phi(r)$ obtained from the electric potential integrated along the trajectories of the incident electrons, i.e., $I_{ph}(r) = \cos[\phi(r)]$.[15] Therefore, we can expect that both the equipotential lines in the reconstructed phase image and the interference fringes in the corresponding hologram are completely blurred when the phase shift $\phi(r)$ varies on the order of π during the exposure time for obtaining a hologram.

Now, we discuss the possible origins of the blurred region with a band shape between the $TaSi_2$ nanowire and anode. First, we investigate the influence of the electrons emitted from the nanowire. In this experiment, when the applied voltage is 50 V, a field-emission current of 0.22 nA is measured. Taking into account this current and a velocity of 300 kV for the incident electrons, both the interaction between the field-emitted electrons and incident electrons and the effect of the electron bombardment on the anode are negligible. In addition, the magnetic field induced by the emitted electrons is too weak to produce a phase shift variation of π. Here, we focus on the electrostatic force drop between the $TaSi_2$ nanowire and anode occurring after a ballistic emission accompanied by a fluctuation in the field-emission current.[8] Figure 3d shows a simulation result obtained on the assumption that the nanowire is positively

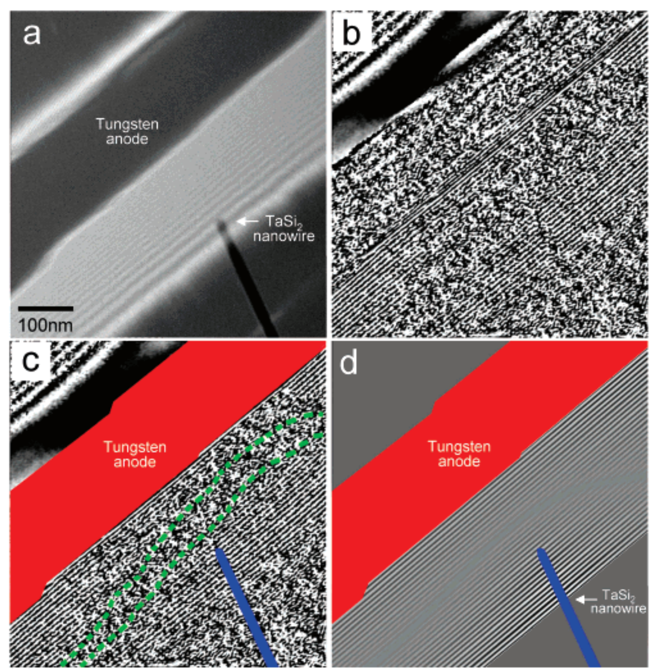

Figure 3. Electron holography result showing the change in electric potential during the field-emission process. Panels a and b show the electron hologram and the corresponding reconstructed phase image of Figure 2c in an enlarged field of view. In (c), the irregular-contrast region is indicated with broken green lines. The $TaSi_2$ nanowire and the tungsten anode are denoted by blue and red colors, respectively. Panel d shows the simulation of the electric potential distribution projected along the incident electrons; this distribution is obtained by taking into account the change in the electric potential in a $TaSi_2$ nanowire during the field-emission process.

charged to be 1.96×10^{-17} C after each ballistic emission; i.e., during each ballistic emission, approximately 100 electrons are emitted from the $TaSi_2$ nanowire. In other words, we assume that the following two states occur during field emission: during a ballistic emission, both the nanowire and its cathode are grounded under the applied voltage of 50 V, while after a ballistic emission, the cathode is grounded but the nanowire is positively charged to be 1.96×10^{-17} C under the applied voltage of 50 V. The simulation was carried out using the method of images on the basis of a one-dimensional line of charge with a complementary image charge distribution.[18,21] It is found that there is a comparable agreement between the simulation and experimental results; i.e., the phase shift variation between the $TaSi_2$ nanowire and anode is evaluated to be π from the simulation. The following discussion is based on the simulation results. In the field-emitting $TaSi_2$ nanowire, a ballistic field-emission process can be reasonably considered, and the interference fringes in the hologram can be completely blurred by a slight change in the amount of charges on the $TaSi_2$ nanowire. On the other hand, the simulation indicates that an electric potential of 1 V was built up in the $TaSi_2$ nanowire due to the positive charges of 1.96×10^{-17} C after each ballistic emission. Consequently, it is inferred that the field emission through a nanowire emitter involves a cyclic process comprising each ballistic emission, the positive charging of the nanowire, and the restoration of electrons in the nanowire. In addition, from the results presented above, we can consider that the potential fluctuation due to the ballistic emission in the nanowire and, probably, other nanostructured emitters such as carbon nanotubes[8] may produce not only a fluctuation in the electron current but also an increase in the energy spread of an electron beam.

Figure 4 shows the electron holography results and $I-V$ curve obtained from the field-emission device using the $TaSi_2$ nanowire with which the field-emission experiments had been carried out approximately 30 times within the transmission electron microscope. The electron holography experiment was performed when the applied voltage and field-emission current were 100 V and 3.2 nA, respectively. In this case, the higher applied voltage (above 80 V) was needed in order to induce the field emission in the $TaSi_2$ nanowire because it was deteriorated by the carbon adsorption (gray contrast region in the nanowire in Figure 4a) during the repeated field-emission process. In addition, we found that the consumption of Ta and Si atoms was accompanied with the field-emission process; the diameter in the $TaSi_2$ nanowire decreased approximately 50% (black contrast region in the nanowire in Figure 4a). From these results, we can suppose that the degradation of a field-emitting $TaSi_2$ nanowire resulted from the consumption of Ta and Si atoms as well as the adsorption of elements such as the residual carbon inside the transmission electron microscope. On the other hand, in the reconstructed phase images of parts b and c of Figure 4, it can be clearly seen that the irregular-contrast region exists under a broken green line except the nanowire position and this is wider than the case shown in Figure 3c. The results indicate

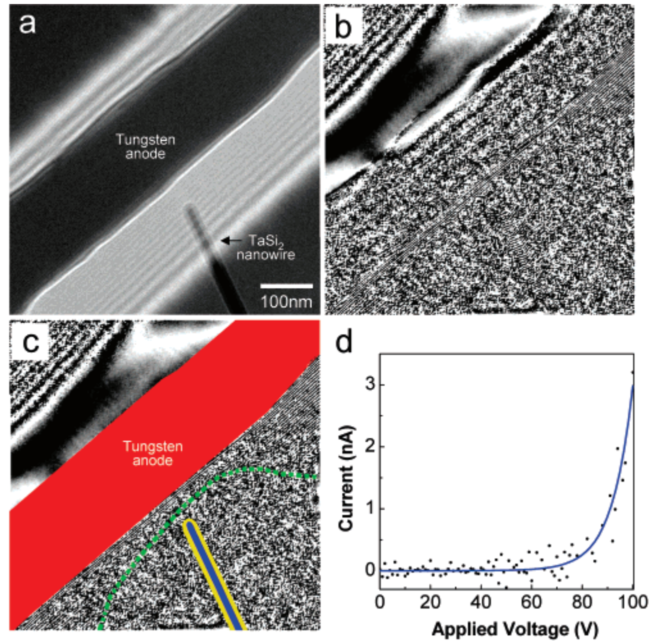

Figure 4. Electron holography results (a−c) and an $I-V$ curve (d) obtained from the field-emitting device using the $TaSi_2$ nanowire with which the field-emission experiments had been carried out approximately 30 times within the transmission electron microscope. Panels a and b show the electron hologram and corresponding reconstructed phase image obtained when the applied voltage is 100 V. In (c), the upper boundary of the irregular-contrast region is indicated with a broken green line. The $TaSi_2$ nanowire and the tungsten anode are denoted by blue and red colors, respectively. The surface contaminated layer formed during the repeated field-emission process is indicated by yellow color.

that the potential fluctuation in the nanowire occurs more severely due to the field-emission process with high electron current.

In conclusion, we have systematically analyzed the field emission properties of a single $TaSi_2$ nanowire within a transmission electron microscope. Through visualizing the electric potential distribution by electron holography, the blurring phenomenon in the hologram resulting from a change in the electric potential in the nanowire during field emission was experimentally observed for the first time. Further, the changes in the field-emission properties and the electric potential in the nanowire due to the surface contamination effect have been discussed. These experimental techniques and results are expected to apply for understanding the properties of various nanostructured field emitters such as carbon nanotubes.

Acknowledgment. This work was partly supported by financial support from Grant-in-Aid for Scientific Research (A) from Japan Society for the Promotion of Science.

References

(1) Gomer, G. *Surf. Sci.* **1994**, *299*, 129.
(2) Baughman, R. H.; Zakhidov, A. A.; De Heer, W. A. *Science* **2002**, *297*, 787.
(3) Rinzler, A. G.; et al. *Science* **1995**, *269*, 1550.
(4) De Heer, W. A.; Châtelian, A.; Ugarte, D. *Science* **1995**, *270*, 1179.
(5) Collins, P. G.; Zettl, A. *Phys. Rev.* **1997**, *B* 55, 9391.
(6) Walker, D. G.; Zhang, W.; Fisher, T. S. *J. Vac. Sci. Technol., B* **2004**, *22*, 1101.

(7) Wang, Z. L. *Adv. Mater.* **2000**, *12*, 1295.
(8) Wang, Z. L.; Gao, R. P.; De Heer, W. A.; Poncharal, P. *Appl. Phys. Lett.* **2002**, *80*, 856.
(9) Bonard, J.-M.; Dean, K. A.; Coll, B. F.; Klinke, C. *Phys. Rev. Lett.* **2002**, *89*, 197602.
(10) De Jonge, N.; et al. *Appl. Phys. Lett.* **2004**, *85*, 1607.
(11) Xu, Z.; Bai, X. D.; Wang, E. G.; Wang, Z. L. *Appl. Phys. Lett.* **2005**, *87*, 163106.
(12) Li, H. J.; Lu, W. G.; Li, J. J.; Bai, X. D.; Gu, C. Z. *Phys. Rev. Lett.* **2005**, *95*, 086601.
(13) Buldum, A.; Lu, J. P. *Phys. Rev. Lett.* **2003**, *91*, 236801.
(14) Cumings, J.; Zettl, A.; McCartney, M. R.; Spence, J. C. H. *Phys. Rev. Lett.* **2002**, *88*, 056804.
(15) Shindo, D.; Oikawa, T. *Analytical Electron Microscopy for Materials Science*; Springer-Verlag: Tokyo, 2002.
(16) Shindo, D. *Mater. Trans.* **2002**, *44*, 2025.
(17) Matteucci, G.; et al. *J. Appl. Phys.* **1991**, *69*, 1835.
(18) Matteucci, G.; Missiroli, G.; Pozzi, G. *Scanning Microsc.* **1997**, *11*, 367.
(19) Chueh, Y. L.; et al. *Nanotechnology* **2007**, *18*, 145604.
(20) Chou, L. J.; et al. *Appl. Phys. Lett.* **2006**, *89*, 023112.
(21) Jackson, J. D. *Classical Electrodynamics*, 3rd ed.; John Wiley & Sons: New York, 1999.

NL070696V